

The Effects of Soil Abrasives on Rotary Seal Effectiveness

by

Hugo M. Ayala

S.B., Mechanical Engineering
Massachusetts Institute of Technology, 1989

Submitted to the Department of
Mechanical Engineering in partial fulfillment of
the requirements for the
degree of

MASTER OF SCIENCE
in
Mechanical Engineering

at the

MASSACHUSETTS INSTITUTE OF TECHNOLOGY

June 1995

©1995 Massachusetts Institute of Technology
All rights reserved.

Signature of Author _____

~~Department of Mechanical Engineering~~
May 12, 1995

Certified by _____

Professor Douglas P. Hart
Thesis Supervisor

Accepted by _____

Professor Ain A. Sonin
Chairman, Departmental Committee on Graduate Studies

MASSACHUSETTS INSTITUTE
OF TECHNOLOGY

AUG 31 1995

LIBRARIES

Barker Eng

The Effects of Soil Abrasives on Rotary Seal Effectiveness

by

Hugo M. Ayala

Submitted to the Department of Mechanical Engineering on
June 1995 in partial fulfillment of the requirements for the
degree of

Master of Science in Mechanical Engineering

Abstract

The tracks of large earth moving equipment manufactured by Caterpillar Tractor Co. often operate in the contact with mud and other abrasive mixtures. These abrasives make their way into the joints of the equipment and accelerate the wear of the moving parts.

This document is a study of the effects of soil abrasives on the seals used in the joints of track vehicles. An experimental setup is described in which a simplified version of a linkage called a bushing assembly is used to reproduce conditions experienced by the seals in the field. Modifications to one of the end caps of the bushing assembly allow measurements of the seal thickness to be performed *in situ*.

Four experiments were conducted in which seals were tested for varying length of time. The results are presented in the form of charts showing the decreasing seal thickness as a function of millions of cycles. Pictures of each of the seals showing the patterns of material erosion are also shown.

Analysis of the data suggest creep and material erosion are major contributors to the change in seal thickness. All seals tested suffered a permanent plastic deformation of 6% from an average seal lip thickness of 1.55 mm. Seals tested with mud became eroded at a rate inversely proportional to the contact area with the bushing. This suggests that seal wear is a function of the contact pressure between the seal lip and the bushing. Finally, an examination of the oil drained from the assembly shows evidence that mud particles are ingested across the seal lip and may become trapped between the seal and the bushing.

Thesis Supervisor: Professor Douglas P. Hart

<back of the abstract>

Biographical Note

Born as the second child in a family of four to Hugo M. Ayala Sandoval and Eugenia J. Vázquez Padua de Ayala on Tuesday September 19, 1967. Attended primary education at Escuela Artículo 123, and seventh through ninth grade at Escuela Secundaria Técnica #8, both located in my birthplace, the small Southeastern city of Minatitlán, Veracruz in México.

For ninth through twelfth grade I enrolled at LaSalle Military Academy, a Military, Catholic, Private school located in Oakdale New York. Attained the degree of Army Cadet Captain and was awarded the Presidential Academic fitness award. Graduated with Gold Honors and First in Achievement In May of 1985.

Enrolled at the Massachusetts Institute of Technology in September 1985. Majored in Mechanical Engineering and did a humanities concentration in Visual Arts. Authored a thesis titled *Design for a Multi-Axial Fringe Stabilizer for Automating the Production of Synthetic Holograms* and graduated with a S.B. in Mechanical Engineering on June 1989. Member of the Pi Tau Sigma Mechanical Engineering Honor Fraternity.

Moved to Palo Alto California and started full-time employment at Apple Computer Inc. on June 1989. Worked on all aspects of Macintosh System Software, but primarily with that having to do with Printing, Graphics, and Typography. Authored portions of the LaserWriter driver and later became a technical lead overseeing the development of the graphics and printing code for the QuickDraw GX System Extension. Was promoted to the level of Senior Engineer in July of 1992.

Left Apple Computer in September of 1994 after completing the QuickDraw GX project and enrolled as a graduate student in the department of Mechanical Engineering at the Massachusetts Institute of Technology.

<back of the biographical note>

Acknowledgments

This work is sponsored by Caterpillar Tractor Company Inc. without whose support this work would not have been possible. In particular, I wish to thank the Chemical Products Business Unit and Alan Dickey, Jerry Metz, Bill Bedford, Don Jackson and the other people with whom I worked with over the last two semesters.

I also wish to thank all of those people with whom I have consulted (not strictly about research) and who have helped me in my work. In particular I wish to thank my drinking buddies Dave, Gregg, Edwin, and Arthur, plus the rest of the folk at the Fluid Mechanics laboratory for listening to my ideas and making life enjoyable; Lisa Tegeler from the Material Properties lab for her help with Abaqus; The technicians and instructors at the Pappalardo Lab, especially Norm and Dick Fenner for imparting their wisdom on how to build things; The staff of the Lab for Manufacturing and Productivity for letting me use their equipment; My brother Héctor for providing technical advice disguised as comic relief; And my father for telling me what was wrong with the electric motor that was driving everyone crazy (and getting it right — among other things).

Finally, and mostly, I wish to thank my advisor, Prof. Hart, for giving me the opportunity to work with him.

<back of the acknowledgments>

Table of Contents

1. Introduction	15
1.1 The D10 Track Seal	15
1.2 Motivation	16
1.3 Previous Research	18
1.4 Scope of this Research.....	18
1.5 Future Research	19
2. Experimental Setup	21
2.1 The Seal Test Unit	21
2.2 The Bushing Assembly.....	21
2.3 Seal Pre-Loading	24
2.4 The Soil Abrasive Mixture	24
2.5 The Mud Containment Box.....	25
2.6 The End Cap Modifications.....	26
2.7 Out of Cavity Seal Measurement	28
3. Theoretical Model.....	29
3.1 Seal Lip Material Properties.....	29
3.2 Seal Lip Geometry	30
3.3 Models of Material Erosion	31
4. Results.....	35
5. Analysis	43
5.1 Seal Lip Creep	43
5.2 Seal Lip Wear	43
5.3 Wear Mechanism	45
5.4 Surface Analysis	46
6. Conclusions.....	49
6.1 Summary of Work.....	49
6.2 Summary of Results	49
6.3 Other Observations	50
6.4 Directions for Future Work.....	50

List of Figures

Figure 1: Two track vehicles manufactured by Caterpillar	15
Figure 2: A cross-section of a track seal.....	16
Figure 3: A cross-section of a linkage.....	17
Figure 4: The Mud Box	22
Figure 5: Detail of the Mud Box showing crank mechanism.....	22
Figure 6: The bushing assembly.....	23
Figure 7: Cross-section of the bushing assembly.....	23
Figure 8: Dimensions for the bushing assembly	23
Figure 9: The clamp and lock-down supports	24
Figure 10: Dimensions for the clamp	25
Figure 11: The mud containment box	26
Figure 12: End cap modifications	27
Figure 13: BTB Measurement detail.....	27
Figure 14: Seal lip modeling	30
Figure 15: Seal lip geometry.....	31
Figure 16: Top of the NCC#1 seal.....	36
Figure 17: Top of the NCC#2 seal.....	37
Figure 18: Bottom of the NCC#2 seal.....	37
Figure 19: Top of the NCC#4 seal.....	38
Figure 20: Bottom of the NCC#4 seal.....	38
Figure 21: Top of the CC#2 seal	39
Figure 22: Bottom of the CC#2 seal.....	39
Figure 23: Top of the CC#1 seal	40
Figure 24: Bottom of the CC#1 seal.....	40
Figure 25: BTB readings for NCC#2	41
Figure 26: BTB readings for NCC#4	41
Figure 27: BTB readings for CC#2	42
Figure 28: BTB readings for CC#1	42
Figure 29: Wear rate for CC#2	44
Figure 30: Wear rate for CC#1	44

List of Tables

Table 1: Possible wear models 33
Table 2: Before and after seal thickness of seals tested..... 36

1. Introduction

At the center of this research is a track shear seal. This document is a study of its design, its use, and chiefly, how it performs under laboratory conditions.

1.1 The D10 Track Seal

The D10 track seal is manufactured by Caterpillar Tractor Co. and is used in the linkages that make up their track-type vehicles. Fig. 1 shows two of the vehicles in Caterpillar's product line that ride on tracks and use seals like the one described in this document.

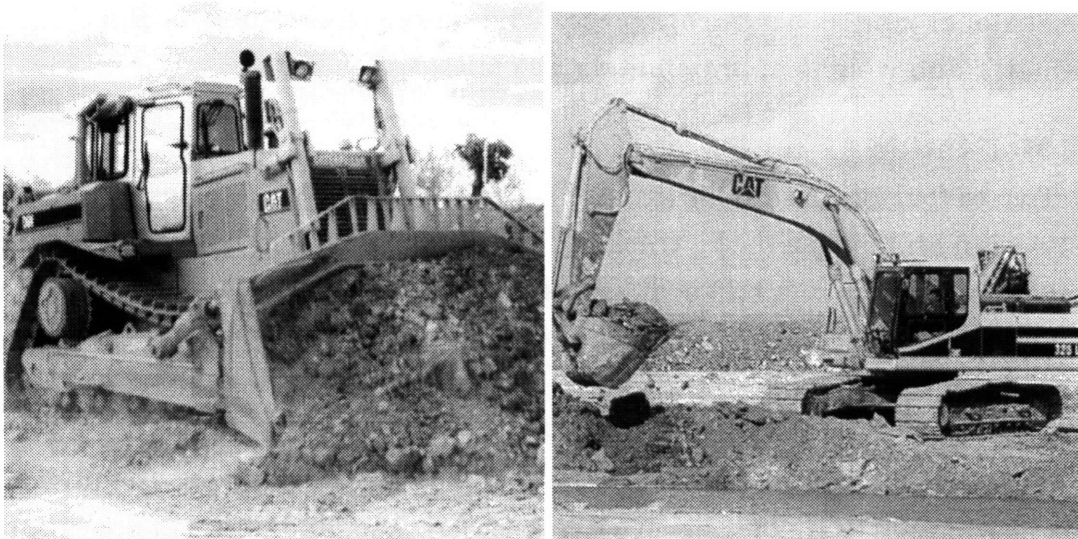


Figure 1: A bulldozer and an excavator manufactured by Caterpillar. Both of these vehicles ride on tracks that use seals like the one that is the subject of this document.

There are three pieces to every D10 seal assembly: the load ring, the stiffener ring, and the seal lip. Fig. 2 shows a cross section of a D10 seal assembly.

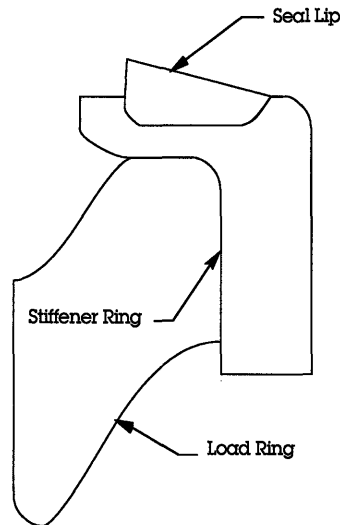


Figure 2: Each D10 seal assembly is made up of the load ring (which is detachable), the stiffener ring, and the seal lip.

The lip is made from a soft polyurethane plastic, and the stiffener ring is manufactured from a much stiffer glass-filled, polycarbonate material. The seal lip is cured directly onto the stiffener ring. The load ring, is manufactured from a nitrate rubber compound, and slips around the base of the stiffener ring as a separate piece. The complete assembly is 10 cm. in diameter and weighs approximately 50 gms.

1.2 Motivation

Two to four of these seals are used in every link of track. Depending on the design and length of the track, there can be anywhere between 160 to 300 seals in one tractor. A two-seal linkage is depicted in Fig. 3.

During normal operation the tractor propels itself by gripping the pin of each of the linkages and rotating it around a sprocket wheel. Because this action is performed without lubrication, the bushings that make up the track undergo severe wear and therefore have to be turned around to the unworn side or completely replaced every two to three thousand hours of operation. During this process, the seals that make up the track are also replaced.

In order to reduce the cost of operating track vehicles, Caterpillar has looked for ways to maximize the numbers of hours of operation between each time that the bushings have to be turned.

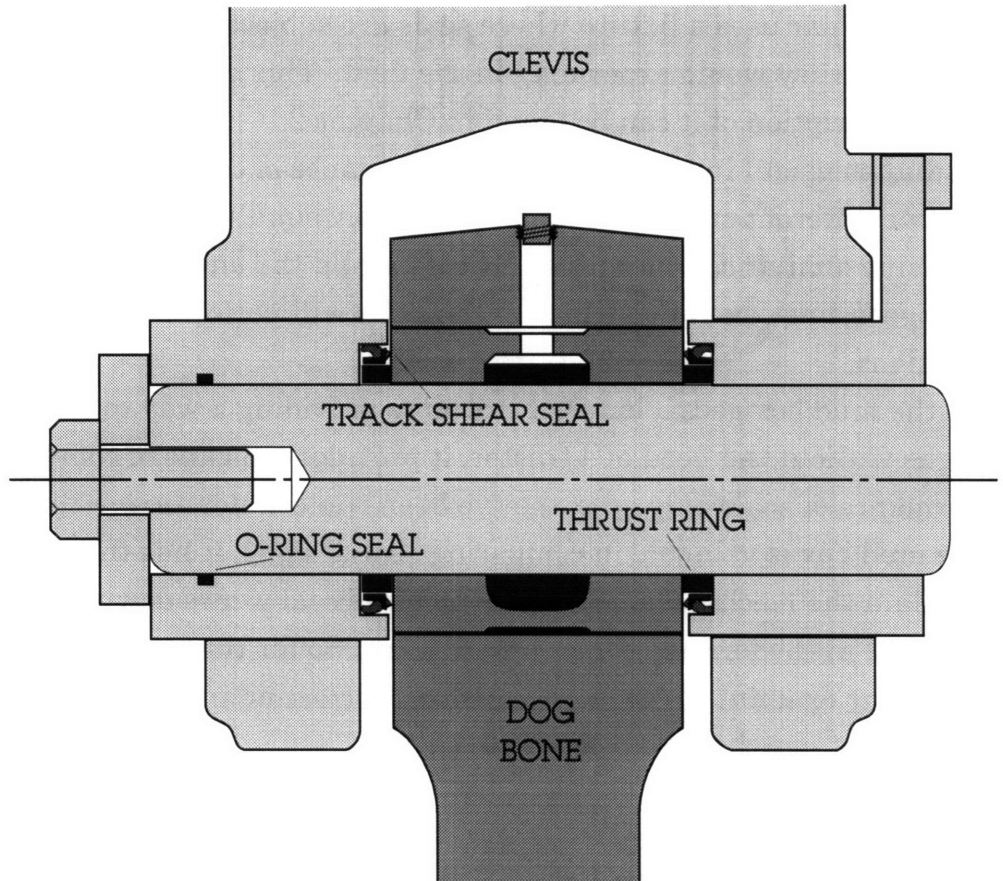


Figure 3: The placement of the seals (two shown in cross section) in a linkage. In addition to their colorful names, the mating ends of two links are identified by different shades of gray.

A new design in which the bushings rotate independently of either link succeeds in prolonging the time of operation. Making the bushings free-rotating substantially reduces the wear they experience thereby prolonging the number of operating hours before the track needs to be disassembled and repaired. However, the seals used in this design are still the same, and they will fail after the same length of time as the ones in the designs where the life of the bushing is the limiting factor. As a result, the life of the seal is now the limiting factor controlling the number of operating hours between maintenance periods, and any change that prolongs their durability, is likely to have a direct effect in the cost of operation.

1.3 Previous Research

Track seals have been the subject of incremental improvements over time. The current D10 design is an outgrowth of several years of fine-tuning in terms of geometry, materials, and assembly configurations. To test these new designs, Caterpillar uses a fixture where seals are subjected to conditions similar to those they would experience in the field. This setup is known as a *mud box*; a description of it can be found in Chapter 2.

This setup is useful in comparing the performance of competing seal designs. Two different seals are installed (possibly simultaneously), and they are worn using similar soil mixtures. By comparing the amount of wear that each undergoes, one can gauge which of the seals will perform better under field conditions.

While the mud box goes a long way towards providing a way to evaluate seal designs without the need of a tractor, it provides a means of comparing the performance of seals only *after* they've been run but not *during* the run. While the mud box is valuable in comparing seal designs, it has thus far not helped explain the mechanism through which the seal wears down in a manner useful in the formulation of new designs. So far this information has been derived by examining the worn seals *post facto*, and inferring from them some theory that matches the observed results.

1.4 Scope of this Research

The ultimate objective of my research is to provide Caterpillar with information to help them extend the time in which the track seals remain effective. In the short term and in the scope of this document, I concentrate on examining methods to perform *in situ* measurement of the erosion of the seal lip material.

In the scope of this document, *seal effectiveness* is taken to be the quality of a seal to function adequately for a given number of hours. Given two seals, the one that functions adequately for a longer period of time when subjected to identical operating conditions is said to have *greater* effectiveness.

For the purposes of this research, seal erosion is the only effect considered to be a factor in seal effectiveness. In particular, a seal is considered to function adequately until its lip has been eroded below a certain threshold.

This research does not account for factors other than seal lip erosion in the role of the seal effectiveness. For example, this research says nothing about

the issue of side loading or *in-play* and what role it plays on seal effectiveness or the effects of oil leakage.

This document does not concern itself with the effects that a change in the geometry or varying soil compositions would have on seal effectiveness. Formulating and verifying a model for the actual wear mechanism, is beyond the scope of this document.

1.5 Future Research

A more in-depth definition and quantification of seal effectiveness is needed; in particular, establishing what range of seal erosion constitutes failure and what other factors contribute to seal effectiveness.

In the long range it should be possible to arrive at a model for how seals of varying geometries and composition become eroded and fail. With this model it should be possible to predict the performance of a seal design in absolute terms and compute an optimal geometry for a given range of operating conditions.

<page 20>

2. Experimental Setup

This chapter describes mud box in which the seals are tested and the modifications and additions required as part of this work. In particular, section 2.5 describes modifications to the bushing assembly end cap which permit *in situ* measurements as the seal is tested.

2.1 The Seal Test Unit

The outermost part of the mud box used for this work is a sheet metal container 12 inches tall by 58 inches long by 19.5 inches wide (see Fig. 4.) Within this enclosure there are two sets of supports each of which can hold a bushing assembly. Fig. 5 shows one of the supports. Fig. 6 shows one of the bushing assemblies, and Fig. 7 shows a cross-section of the bushing assembly.

2.2 The Bushing Assembly

The bushing assembly is a simplified version of the track joint depicted in Fig. 3. The bushing represents the linkage extending downwards, and the pin plus the end caps serve as the link extending upwards. The dimensions of the pin and bushing are shown in Fig. 8.

The bushing assembly is has four individual components. The innermost part is called the *pin*. It is the place against which the two end caps are bolted, and around which the bushing rotates. The pin has a hollow center which serves as an oil reservoir. The clearance between the bushing and the pin is .5 mm.

The space between the end cap and the bushing where the seal are mounted in called the *seal cavity*. When mounted in the bushing assembly, seals are oriented so that the part number imprinted on the back of the

stiffener ring aligns with the 12 o'clock position (the *top* of the seal.) This consistency in alignment permits a uniform comparison of the seal lip across a series of experiments.

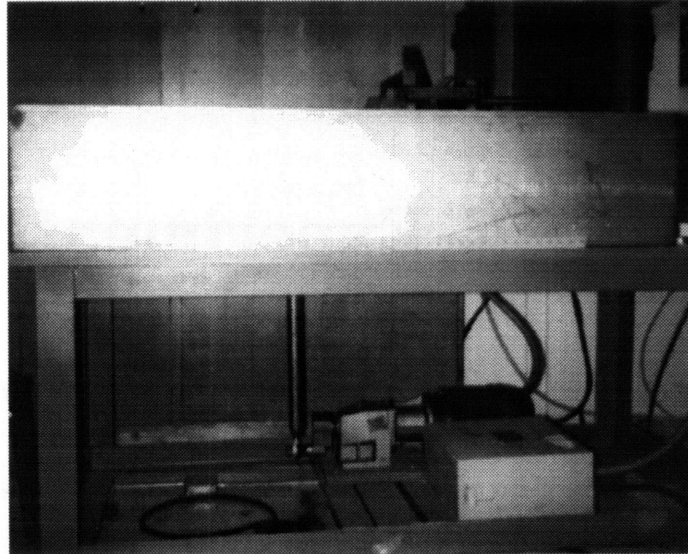


Figure 4: The outermost part of the mud box. Visible in this picture is the table support, the electric motor, a three phase transformer, and the box housing the control unit.

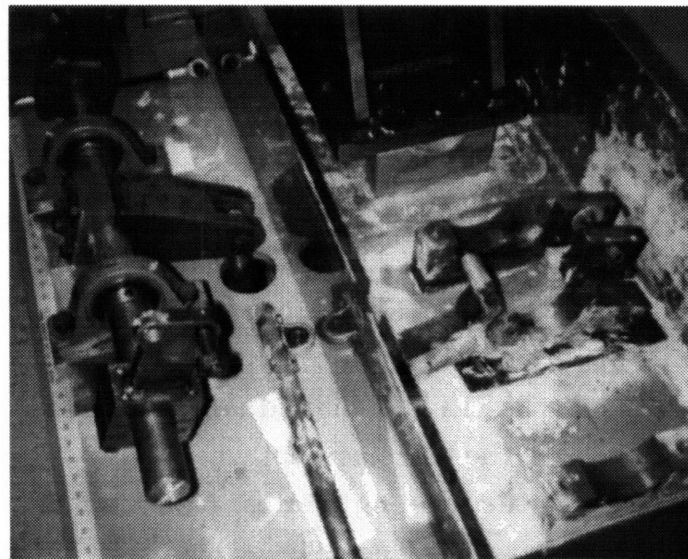


Figure 5: The inside of the mud box. On the left is one of the pairs of supports that holds the bushing assembly as it is being tested. on the left is the crank that drives the clamp that turns the bushing assembly.

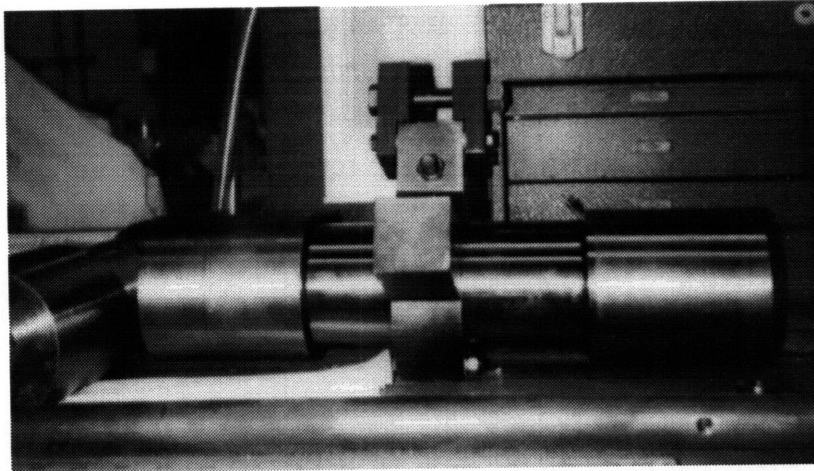


Figure 6: The bushing assembly is shown outside of the mud box with the clamp used for rotating the bushing attached. The two end caps remain stationary while the clamp rotates the pin back and forth by 37° of revolution.

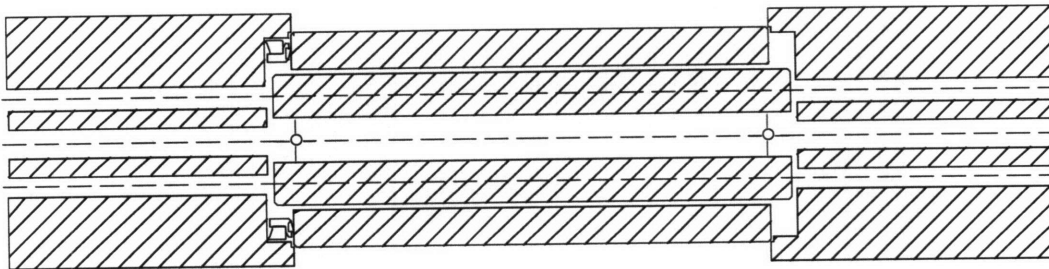


Figure 7: A cross section of the bushing assembly in which the D10 seals are tested. The D10 seal is shown only in the left side of the assembly.

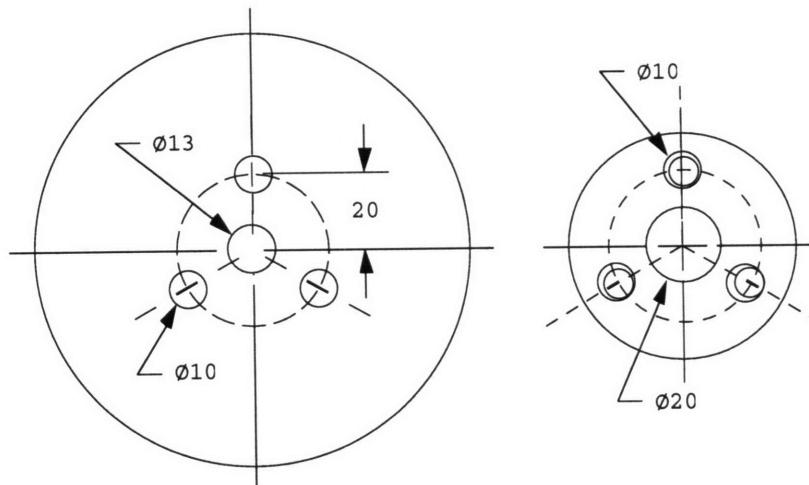


Figure 8: A schematic showing the dimensions of the cap and of the pin that connects the two end caps.

The two end caps are bolted down solid against the pin. The bushing assembly is bolted down to the supports around the end caps. Each of the end caps hold one seal with the seal lip pressed against the bushing.

While the set up is operating, a clamp rotates the bushing by 37° degrees of arc (see Fig. 9 & 10.) The rate at which the pin is rotates is chosen as 9 cycles every ten seconds. This replicates the frequency of a moving tractor. One back and forth motion translates the face of the bushing against the seal by approximately 26 mm.

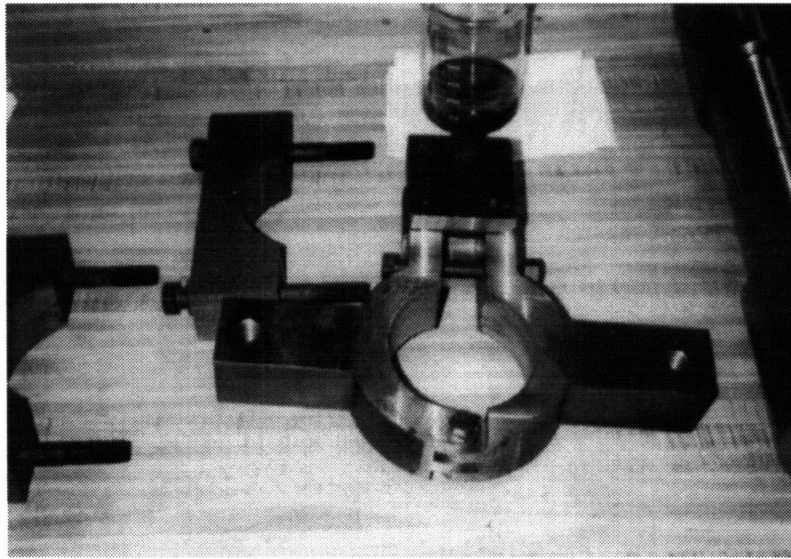


Figure 9: This picture shows the clamp used to rotate the bushing.

2.3 Seal Pre-Loading

The pin and the bushing are constructed so that they differ in length by 22.6 mm. Because the end caps are bolted solid against the pin, the combined length of the seal cavities always remains constant at 22.6 mm.

Two identical seals mounted in opposing seal cavities would each be compressed from their natural length of 15.5 mm, to 11.3 mm (i.e., half the difference in length of the bushing and the pin.)

2.4 The Soil Abrasive Mixture

During the test the bushing assembly is submerged in a mud bath. The mud is a mixture (by weight) of 29.47% fire-clay, 39.30% bank sand, 0.21% Cabosil/Hysil, 0.14% salt, and 30.88% water. This is the same mixture that is used by Caterpillar and was used in all of the experiments without alteration.

The mixture is representative of the field conditions encountered by the tractors.

For this research a mixture of three parts water and five parts dry solids (by volume) was used as a starting point in all experiments. The effect of the water evaporation on the mixture was minimized by daily re-mixing.

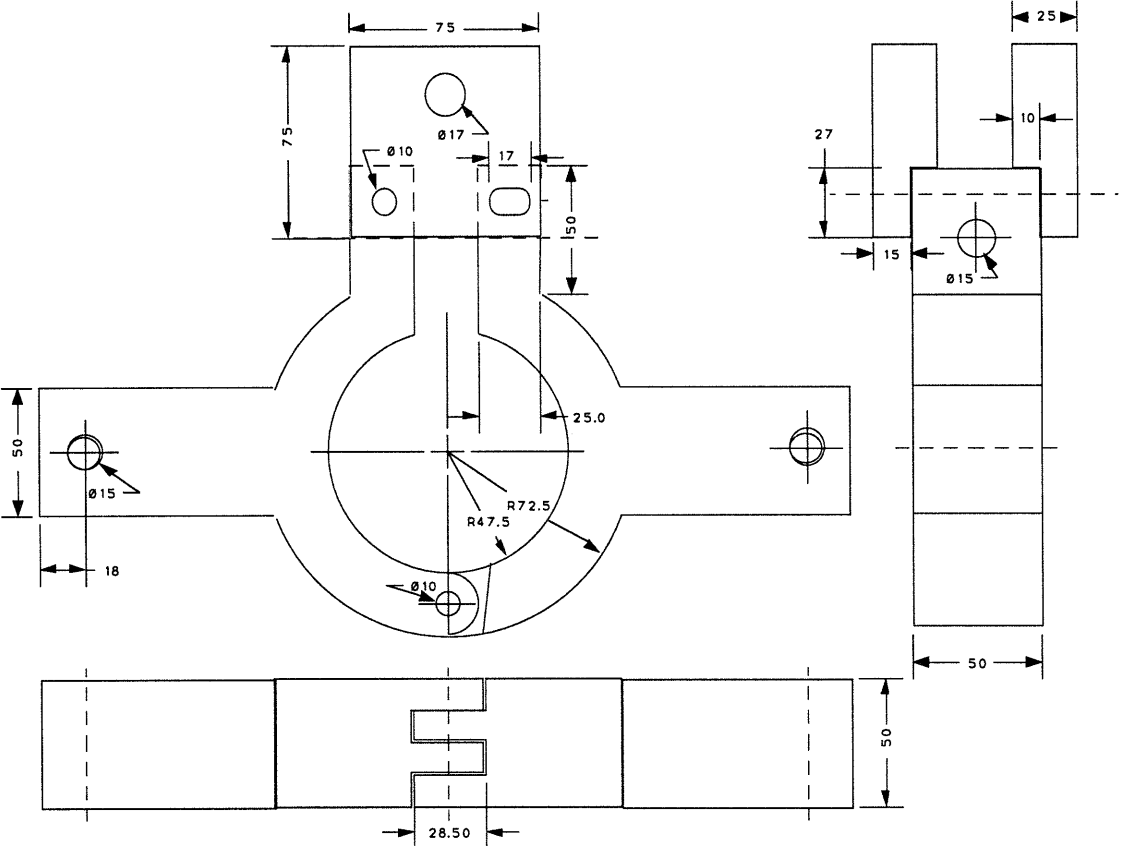


Figure 10: A schematic showing the dimensions of the clamp. All dimensions are in mm.

2.5 The Mud Containment Box

As is, each tank requires about 10 gallons of dry solids and 6 gallons of water to completely submerge a pin bushing assembly. In order to improve the consistency of the mud that the seals were tested with, an attachment was designed to confine the mixture to the gap between the seal and the bushing. This attachment (shown in Fig. 11) is about the size of a cereal box, and requires 2 quarts of mud to cover the assembly.

One problem with the containment box is that it leaks mud on the side of the rotating bushing. This means that the top of the bushing assembly inside

the box will sometimes become exposed to air. The effects of this have not yet been quantified. However, since the same thing happens when ten gallons of mud are used, no advantage is lost in using this fixture.

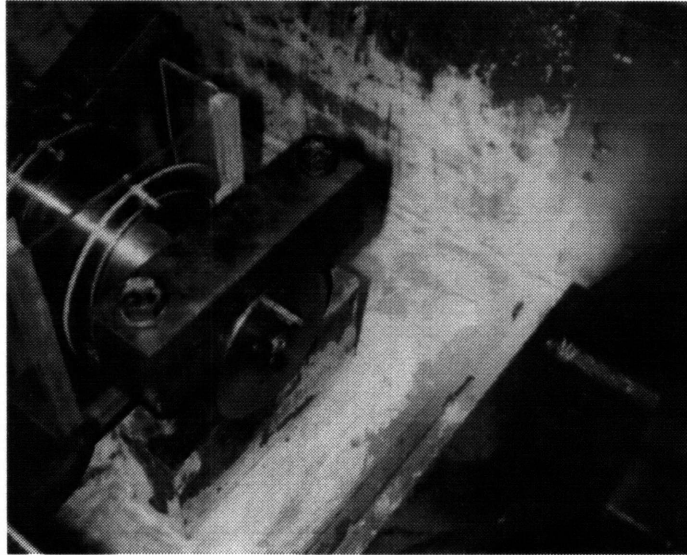


Figure 11: The attachment used to contain the mud mixture around the gap between the end-cap and the bushing is shown in the upper left part of this picture. The container is empty of mud.

2.6 *In situ* Seal Measurement

A hole was drilled through one of the end caps so that four steel rods could be inserted to relay information on seal position and thickness. The hole is placed so that two of the steel rods contact the back of the stiffener ring, and the other two contact the bushing. Each one of the stainless steel rods is 140 mm in length and 1/64 of an inch in diameter.

The distance between the base of the stiffener ring and the bushing is referred to as the BTB (base-to-bushing) measurement. Fig. 13 shows the three measurements that are used in computing the BTB and the error. First, the distance between the back of the end cap and top rods (those contacting the back of the stiffener ring) is measured. This is labeled A. Next the distance between the end cap and the bottom rods (those contacting the face of the bushing) is measured. This is labeled B. Finally, the difference between the top rods and the bottom rods is measured. This is labeled C.

These measurements allow for one level of redundancy on the seal lip estimate and provide information about the absolute position of the seal and the bushing with respect to the end cap. Knowing the absolute positions is

useful in estimating the load on the seal at the time of the measurement. Section 3 describes how these measurements are translated into estimates of seal lip wear.

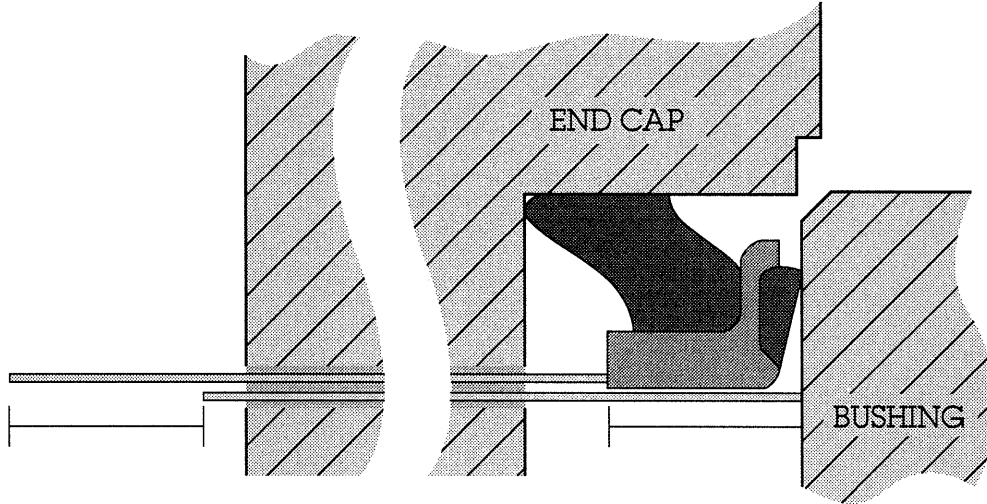


Figure 12: The placement of the steel rods used in *in situ* measurement are shown. The difference in length between the rods conveys the distance between the back of the stiffener ring and the bushing. From this measurement the thickness of the seal lip can be estimated.

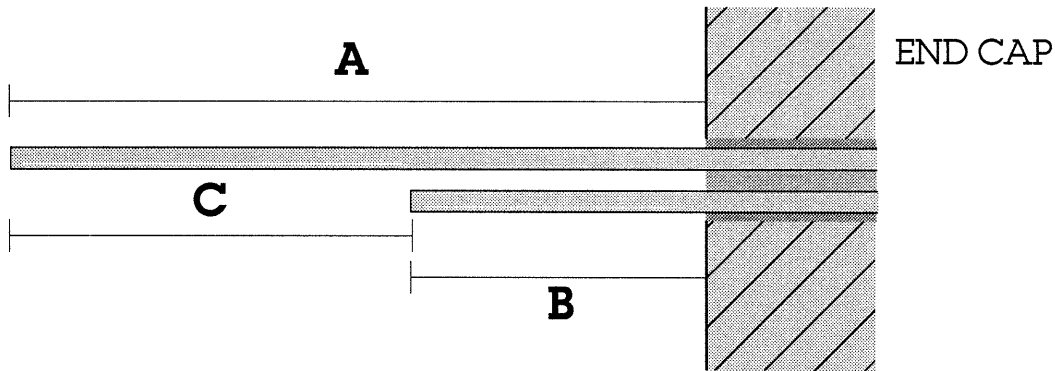


Figure 13: Every reading consists of measuring three values. The first (A) is the distance between the back of the end-cap and the rod that contacts the back of the stiffener ring. The second (B) is from the end cap to the rod that contacts the bushing. The last (C) is the difference between the two rods.

2.7 Out of Cavity Seal Measurement

Measuring the dimensions of the seal outside of the seal cavity is complicated because of the small features and slants of all the faces of the seal lip and stiffener ring. For this reason, a stand that holds the seal lip perpendicular to a flat plate was constructed. The distance between the back

of the stiffener ring and the plate can then be measured consistently. Out of cavity seal measurements reported in section 4 were taken using this stand.

3. Theoretical Model

The interpretation of experimental readings is complicated by the visco-elastic nature of the seal lip material and its geometry.

The end cap modification described in section 2.6 and the BTB readings obtained from it are designed to isolate changes in the seal lip from the rest of the seal assembly. In particular, the BTB readings are meant to be an indicator of changes in seal lip thickness due to material erosion.

Three objects are involved in the BTB measurement: the steel rods used to contact the seal and the bushing, the seal stiffener ring, and the seal lip. The stiffener ring is known to deform *during* the loading of the bushing assembly; but for the purposes of interpreting the BTB measurements, it is assumed that the stiffener ring does not deform appreciably *after* the seal has been loaded. Similarly, the steel rods are assumed to be sufficiently stiff that they do not deform during the taking of the reading.

3.1 Seal Lip Material Properties

The seal lip, on the other hand, can contribute to the BTB reading in one of three possible ways: wear, elastic deformation, and permanent plastic deformation (creep.)

As material is eroded away from the seal, the seal lip moves in closer to the bushing and the BTB readings go down. However, the presence of foreign particles (e.g., mud) between the seal and the bushing can interfere with the readings by lessening or reversing their expected decrease with time. There is no clear way to account for this other than to assume that it is impossible for the seal to spontaneously reconstitute and that any rise in the BTB

readings is due to particles (mud or otherwise) being trapped between the seal and the bushing.

Finally, as stated in section 2.3, when the seal is compressed from its natural length of 15.5 mm to about 11.3 mm, some of the deformation is taken up by the seal lip while most of it is taken up by the load ring.

Fig. 14 shows a model for the seal as a combination of a dash pot and a spring. The spring in the model accounts for the resiliency of the seal lip and the dash pot accounts for the irreversible plastic deformation (creep) that the seal lip experiences.

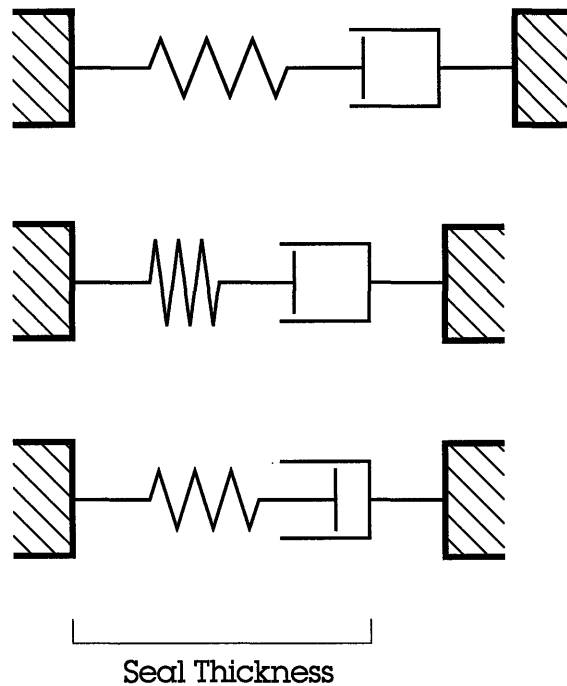


Figure 14: The three pictures shown represent the state of the system before loading (top), immediately after loading (middle), and after the seal has undergone permanent plastic deformation (bottom). Each seal is modeled as a spring and a dash pot.

The effects of this deformation on the BTB can be subtracted by taking a set of readings for a run without the presence of soil abrasives. The BTB readings for that run reflect changes in the seal thickness due to the visco-elastic properties of the seal material.

3.2 Seal Lip Geometry

Fig. 15 shows a detail of the seal lip geometry. The angle of the two faces as well as the dimension of the base of the seal are used to specify the

geometry. The quantity $h(t)$ is the seal thickness (the part of it that rises above the stiffener ring and which is subject to erosion) given as a function of time (here measured in millions of cycles.) A BTB reading is a measure of $h(t)$ offset by the distance between the base of the bushing and the seal lip.

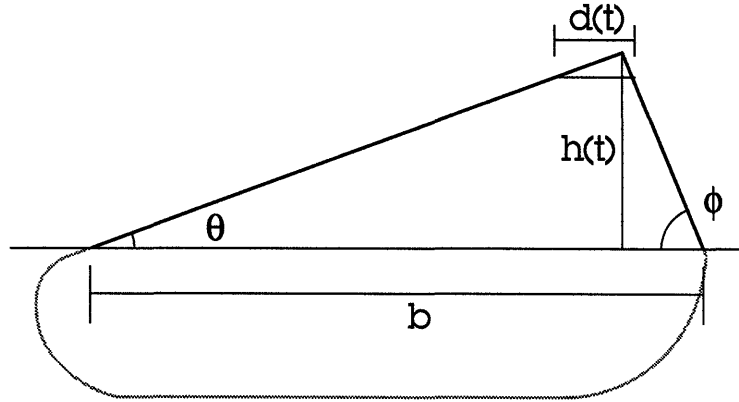


Figure 15: The seal lip geometry is described by three quantities: the two angles θ and ϕ , and the base dimension b . As the seal wears over time, the seal thickness $h(t)$ goes down and the surface of the seal in contact with the bushing $d(t)$ goes up.

3.3 Models of Material Erosion

As material is eroded from the seal, the amount of the seal lip that is in contact with the bushing increases. The quantity $d(t)$ can be related to the seal thickness as follows:

$$\alpha = \frac{1}{\tan \theta + \tan \phi} \quad (1)$$

$$h_0 = \alpha \cdot b \quad (2)$$

$$d(t) = \alpha \cdot (h_0 - h(t)) \quad (3)$$

where h_0 represents the original seal thickness, and α is a function of the geometry of the seal lip.

What is to be determined is the rate at which the seal wears. That is, the time rate of change of $h(t)$. Three possibilities are considered:

$$-\frac{dh(t)}{dt} \propto 1 \quad (4)$$

$$-\frac{dh(t)}{dt} \propto d(t) \quad (5)$$

$$-\frac{dh(t)}{dt} \propto \frac{1}{d(t)} \quad (6)$$

Eqn. 4 is the case where the rate of seal erosion is constant. In this case the BTB readings would appear along a line of decreasing slope when plotted. In physical terms, this represents an increasing amount of material being transported from the seal lip interface as time progresses. That is, as more of the seal comes in contact with the bushing, an increasing volume of the seal lip is eroded and $h(t)$ decreases linearly.

Eqn. 5 is the case where the rate of seal erosion is proportional to the amount of seal in contact with the bushing. The smaller the contact surface, the less wear the seal incurs and vice-versa. As with the first equation, this requires that the volume being eroded with time increase as time progresses. In analytical terms this corresponds to a solution where the seal thickness decreases as one minus an exponential term, and the volume of the seal being eroded increases exponentially with time. If this is the case, a plot of the BTB measurements would show a slow rate of wear at the beginning followed by a gradually accelerating fall.

Finally, Eqn. 6 corresponds to the case where the rate of seal erosion is inversely proportional to the seal surface. In physical terms this would correspond to large rates of wear occurring at the beginning (when the seal lip contacts with the bushing through a thin band), and slower rates of wear later (as the band grows thicker). This case also corresponds to a constant volume of the seal being eroded and transported away per unit time. BTB readings would appear along a the curve of a square root in this case.

Table 1 is a summary of the possibilities considered.

Relation	Solution	BTB Plot	Description
$-\frac{dh(t)}{dt} \propto 1$	$h(t) = h_o - k \cdot t$		Seal thickness decreases linearly with time.
$-\frac{dh(t)}{dt} \propto d(t)$	$h(t) = h_o - k \cdot e^{\alpha t}$		Seal thickness is proportional to the seal contact area.
$-\frac{dh(t)}{dt} \propto \frac{1}{d(t)}$	$h(t) = h_o - k \cdot \sqrt{\alpha t}$		Seal thickness is inversely proportional to seal contact area.

Table 1: Summary of possible seal wear mechanism and corresponding expected measurements. The first column shows a differential equation relating the seal thickness $h(t)$ and the seal contact area $d(t)$. The second shows the solution for $h(t)$ (h_o is the initial seal thickness and k is the wear rate – to be determined.) The graphs show what a plot of BTB measurements (described in section 2.6) would look like if the relationship holds.

<page 34>

4. Results

A total of four experiments were performed as described in section 2. Each of the seals used in the test was given a label that identifies it uniquely, either CC or NCC followed by a number (standing for Caterpillar Control, or New Caterpillar Control.) Table 2 is a summary of the duration of each test and the before and after out-of-cavity measurements for each seal and counter-seal used in the experiments (i.e., seal thickness measured under zero-load conditions.) The top and bottom of each seal tested was photographed under 17x magnification. Fig. 16 through 18 show a seal and a counter-seal tested without mud. Fig. 17 through 24 show the top and bottom of two seals tested with mud. Observations about these pictures are the subject of section 5.4.

Fig. 25 through 28 are plots showing the BTB measurements for each of the runs. The horizontal axes is given as the number of cycles in millions and the vertical as the BTB measurement in millimeters. The conversion between the hours of operation (as recorded) and the millions of cycles was done assuming 9 cycles every ten seconds (see section 2.2.) One million cycles take 13 days to complete.

The BTB value plotted on the vertical axis is the average of the two redundant ways of measuring the BTB distance (see Fig. 11). The error bars are given by extending a line from the average to the two measurements. Included in the plot is the BTB for the unloaded seal at the beginning and the end of the test. This measurement was taken with the bushing assembly resting vertically and with the end cap unbolted but still resting on the seal.

Finally, note that the starting point for the plot shown in Fig. 27 is about .2 mm higher than the other plots. This is because a slightly shorter rod was used to contact the bushing. Had the same rod been used in all tests, all of the initial BTB measurements for seals under load would've been right around 10.2 mm.

Whenever possible, the data and the figures are ordered by the duration of the test, with the shortest tests shown first.

cycles (M)	mud	m-seal	bef. (mm)	aft. (mm)	c-seal	bef. (mm)	aft (mm)
0.53		NCC#2	10.85	10.76	NCC#1	10.87	10.76
0.53	•	NCC#4	10.83	10.71	NCC#3	10.83	10.76
0.94	•	CC#2	10.83	10.70	CC#4	10.84	10.73
1.06	•	CC#1	10.86	10.64	CC#7	10.85	10.74

Table 2: The before and after dimensions of the measured seal (m-seal) and the counter seal (c-seal) used in each of the four experiments is shown as a function of the length of the test (in millions of cycles) and the presence of mud.

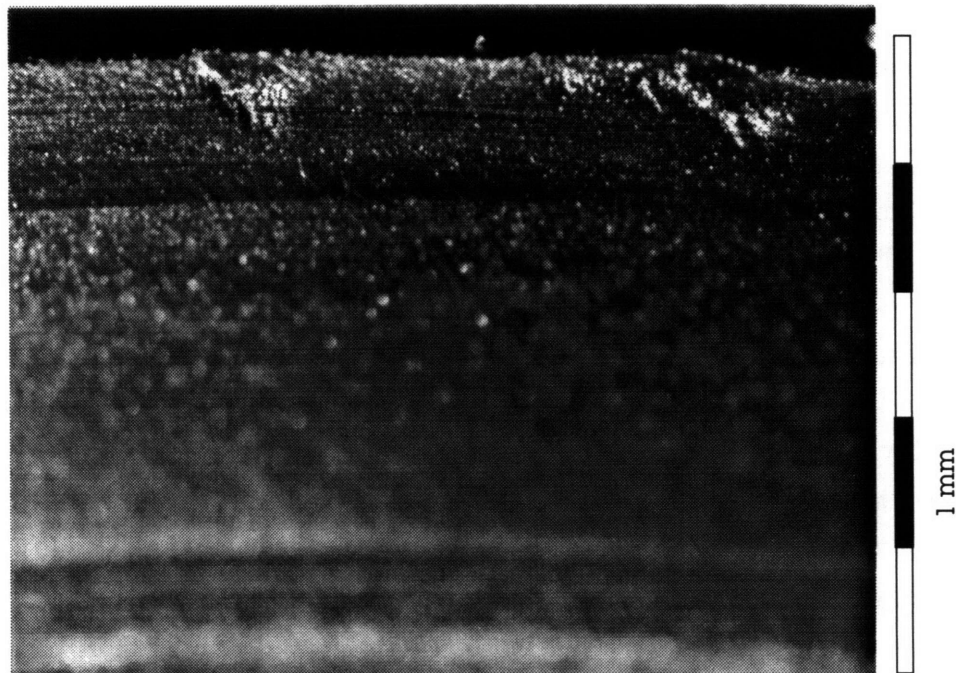


Figure 16: The top of the NCC#1 seal (worn counter to NCC#2). Tested without mud for .53 million cycles. Magnification 17x.

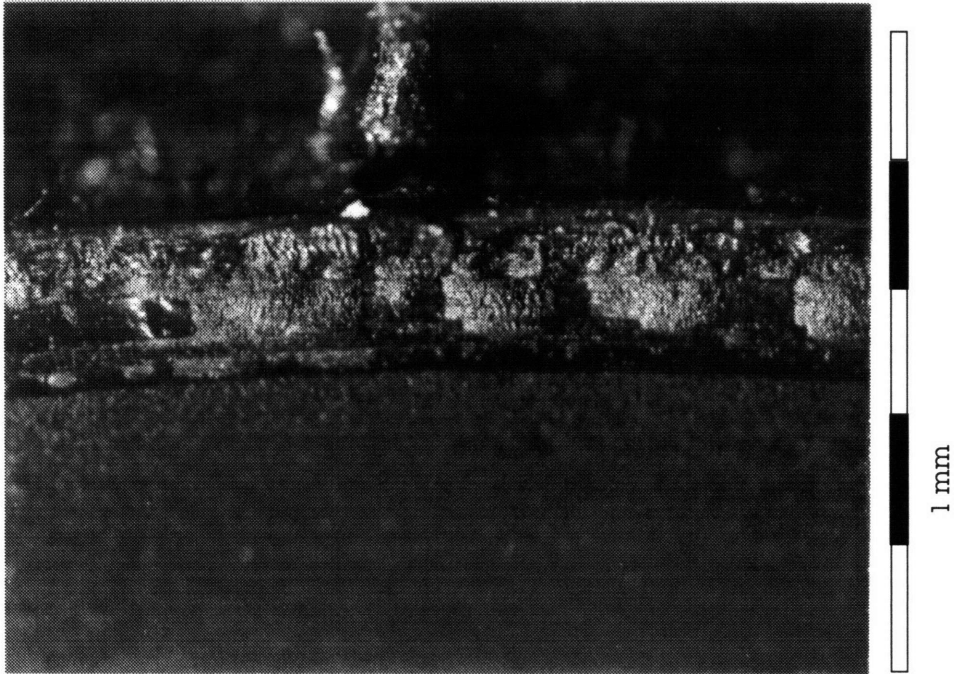


Figure 17: The top of the NCC#2 seal. Worn without mud for .53 million cycles. Magnification 17x. The measurements for this run are Fig. 25.

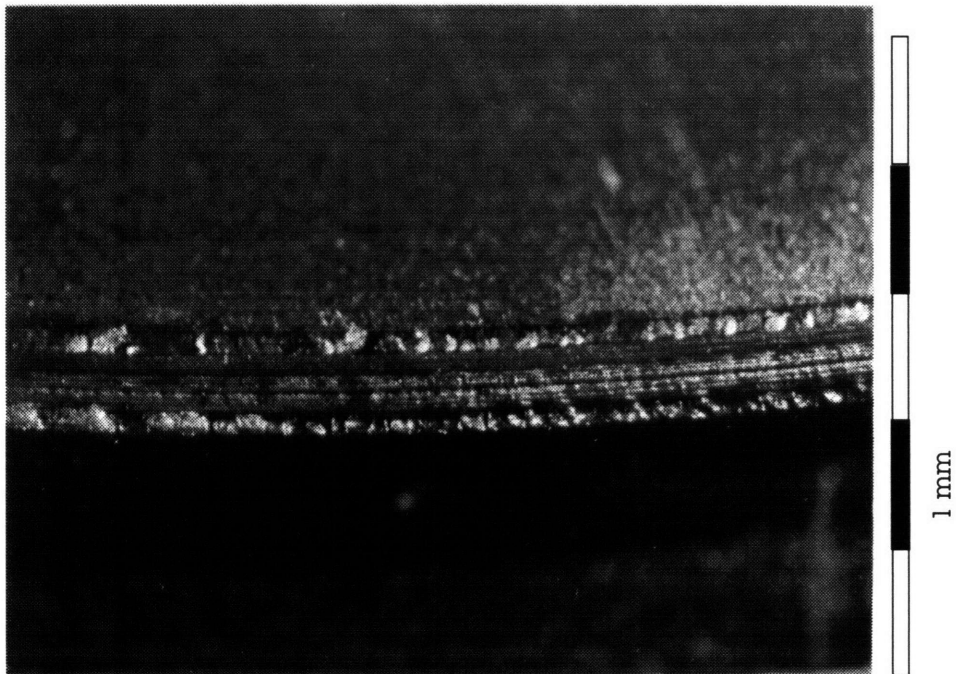


Figure 18: The bottom of the NCC#2 seal. Worn without mud for .53 million cycles. Magnification 17x. The top of the seal is shown above.

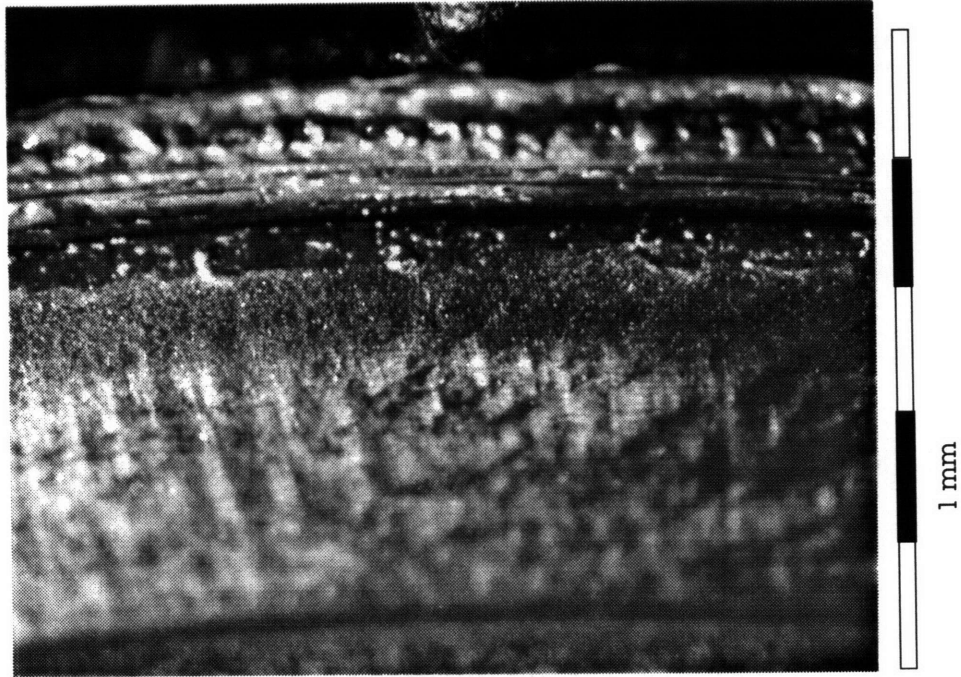


Figure 19: The top of the NCC#4 seal. Worn with mud for .53 million cycles. Magnification 17x. The measurements for this run are shown in Fig. 26.

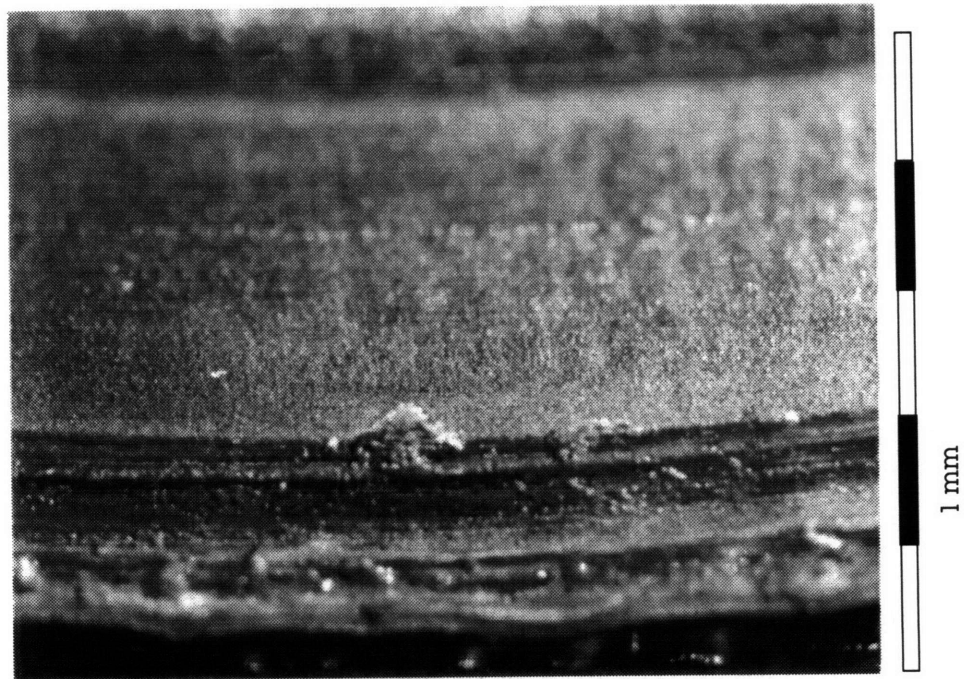


Figure 20: The bottom of the NCC#4 seal. Worn with mud for .53 million cycles. Magnification 17x. The top of this seal is shown above.

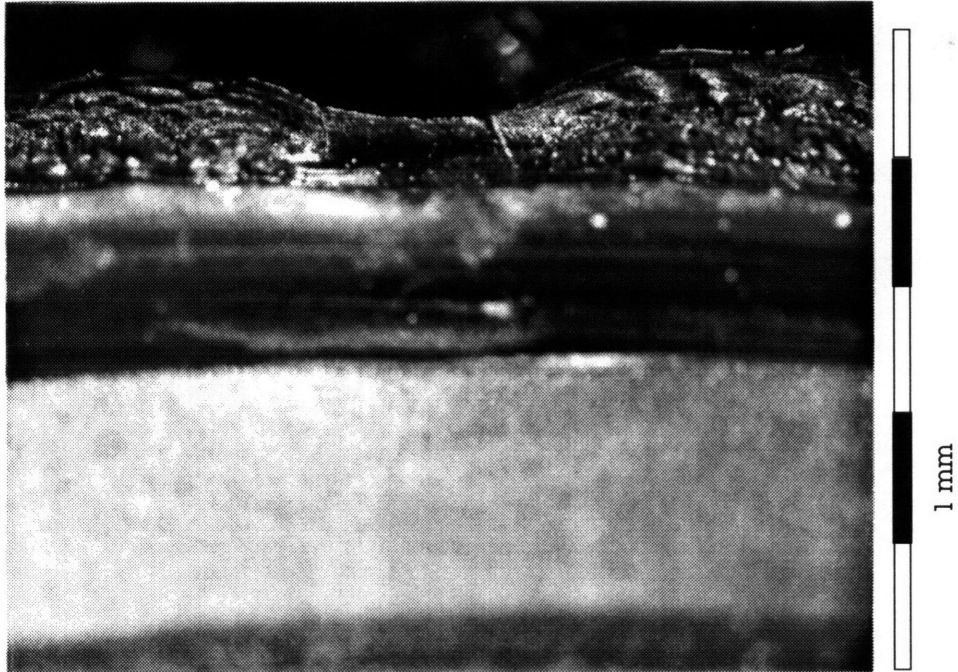


Figure 21: The top of the CC#2 seal. Worn with mud for .94 million cycles. Magnification 17x. The measurements for this run are shown in Fig. 27.

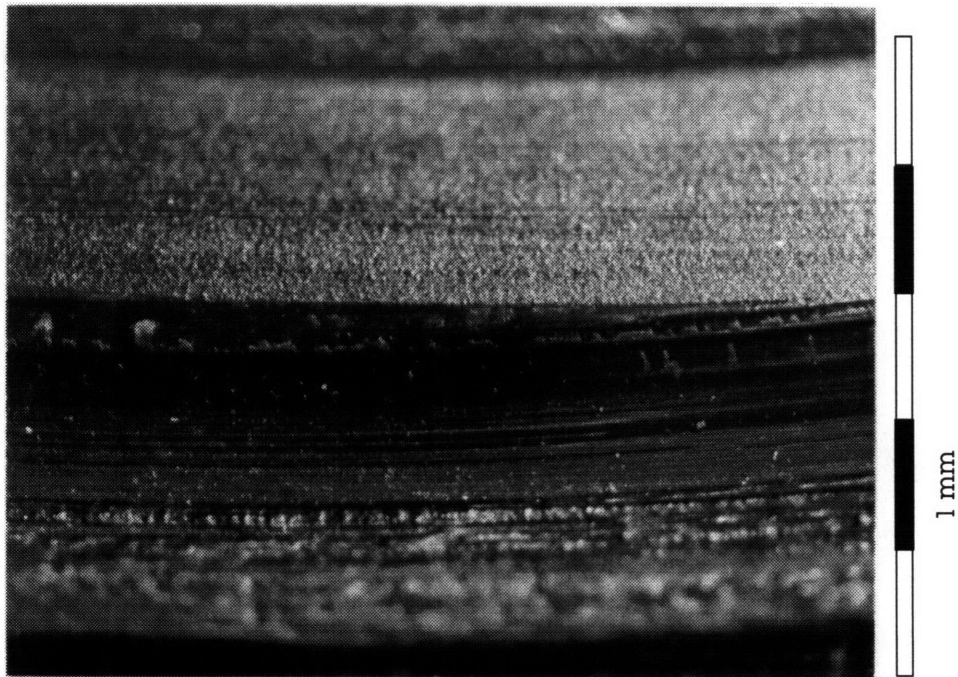


Figure 22: The bottom of the CC#2 seal. Worn with mud for .94 million cycles. Magnification 17x. The top of this seal is shown above.



Figure 23: The top of the CC#1 seal. Worn with mud for 1.06 million cycles. Magnification 17x. The measurements for this run are shown in Fig. 28.

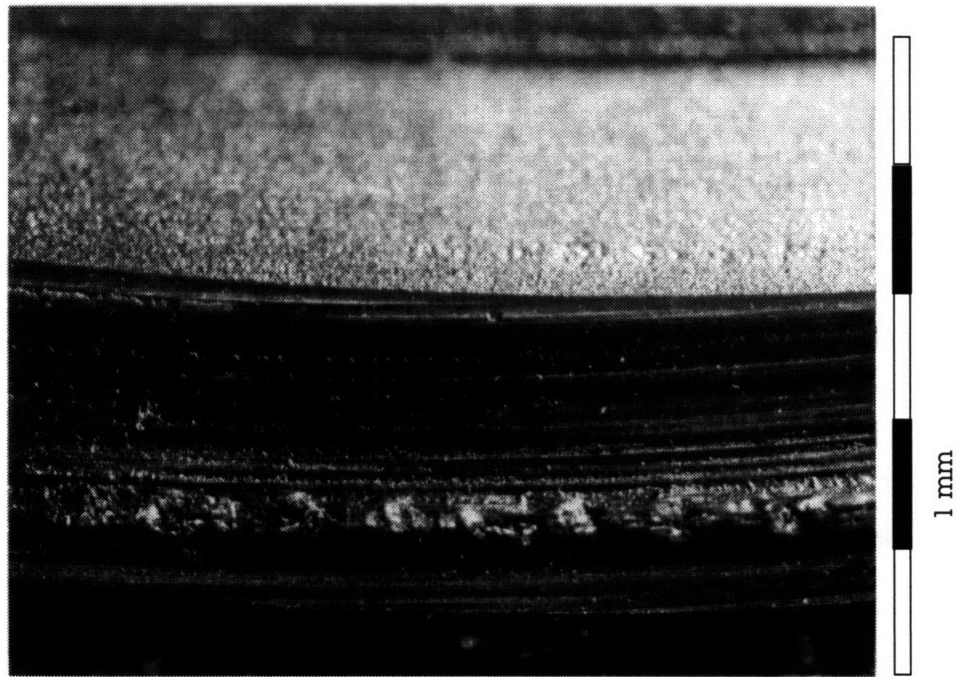


Figure 24: The bottom of the CC#1 seal. Worn with mud for 1.06 million cycles. Magnification 17x. The top of this seal is shown above.

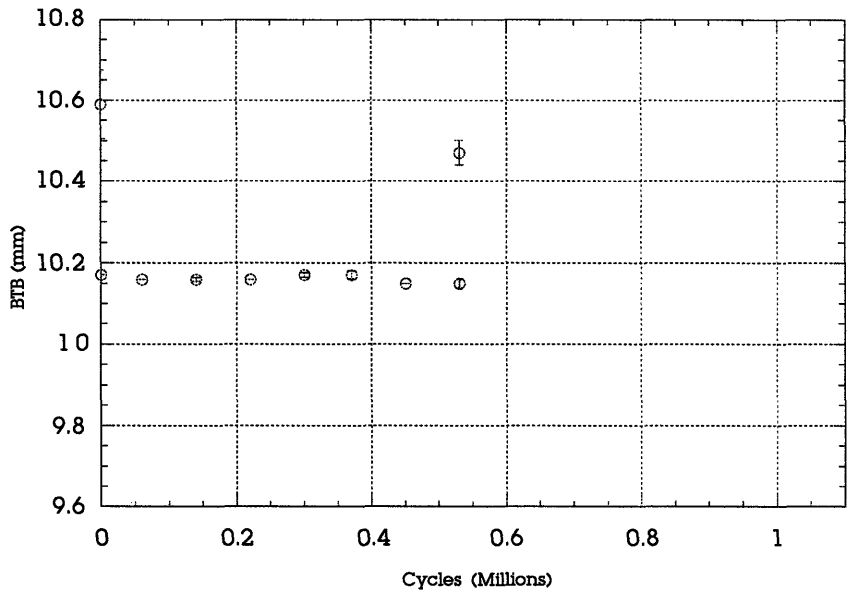


Figure 25: A plot of the BTB measurement for seal NCC#2. This seal was run without mud. The first and last data points correspond to the unloaded seal.

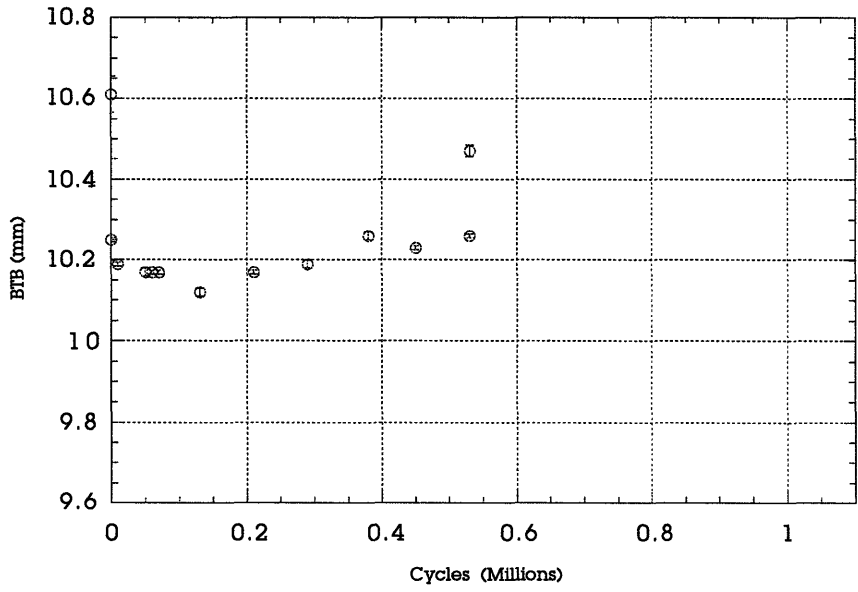


Figure 26: A plot of the BTB measurement for seal NCC#4. This seal was run with mud. The first and last data points correspond to the unloaded seal.

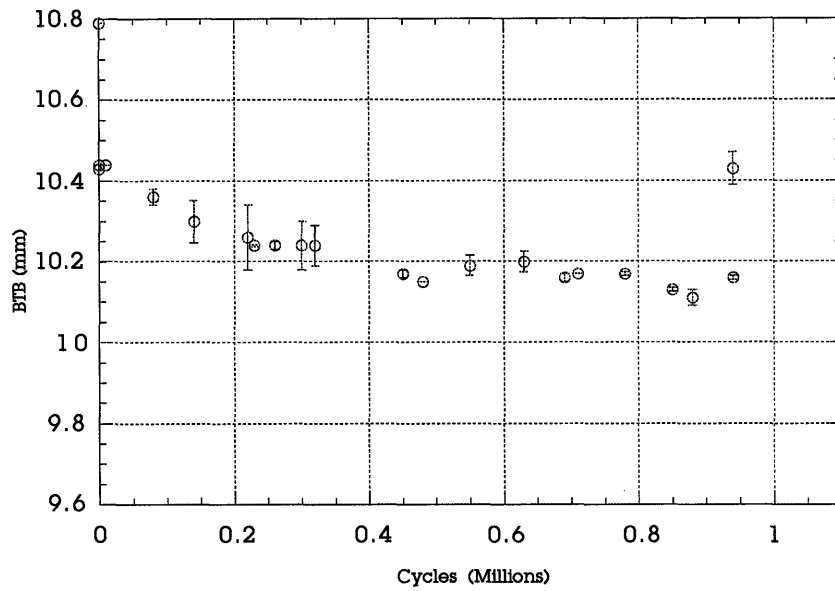


Figure 27 A plot of the BTB measurement for seal CC#2. This seal was run with mud. The first and last data points correspond to the unloaded seal.

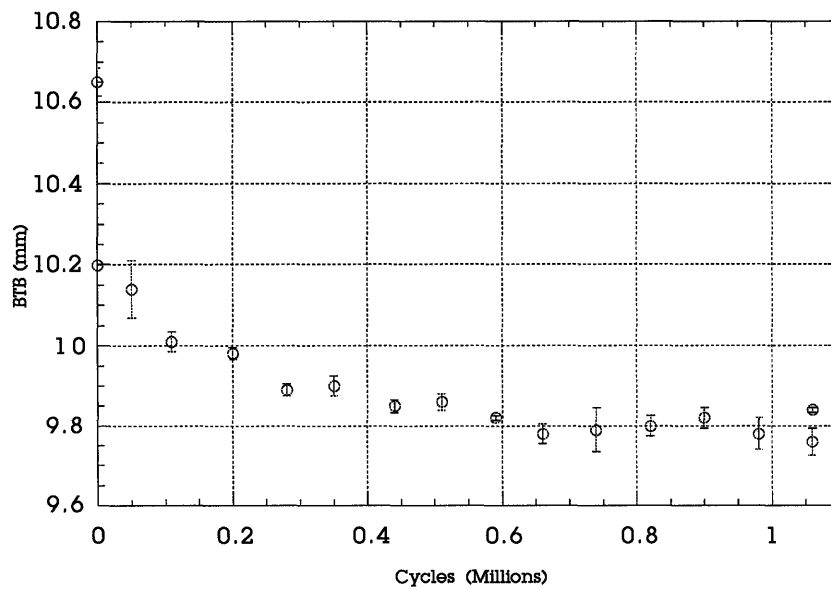


Figure 28 A plot of the BTB measurement for seal CC#1. This seal was run with mud. The first and last data points correspond to the unloaded seal.

5. Analysis

There are three steps in analyzing the data collected. First the effects of creep and the seal elastic deformation and their influence on the BTB reading are analyzed. From this analysis the BTB readings are adjusted in order to isolate the seal wear component. Next the data is analyzed to see what wear mechanism it represents (see section 3.3.) Finally, the wear rates for the experiments run are computed.

5.1 Seal Lip Creep

The before and after readings in Table 2 show that every seal run without mud suffers a permanent plastic deformation of between .07 and .11 mm.

The data plotted in Fig. 25 and the readings taken for the CC#2 run shows that the effect of any permanent plastic deformation is complete in a matter of hours, certainly by the time a day has gone by. Since the time that it takes for the creep to set in is much shorter than the time it takes for material to be eroded from the seal, BTB readings of experiments using mud can be used unchanged. If the creep had set in over a longer period (e.g., seven days), the BTB readings for those days in other runs require an adjustment to have the effect of creep removed.

5.2 Seal Lip Wear

The shape of the curve for seals CC#1 and CC#2 (Fig. 27 & 28) suggest that the seal wear is inversely proportional to the surface of the seal exposed (Eqn. 6). The variable $w(t)$ is introduced as a complimentary quantity to $h(t)$ that represents the amount of the seal lip worn as a function of time. It is defined as follows:

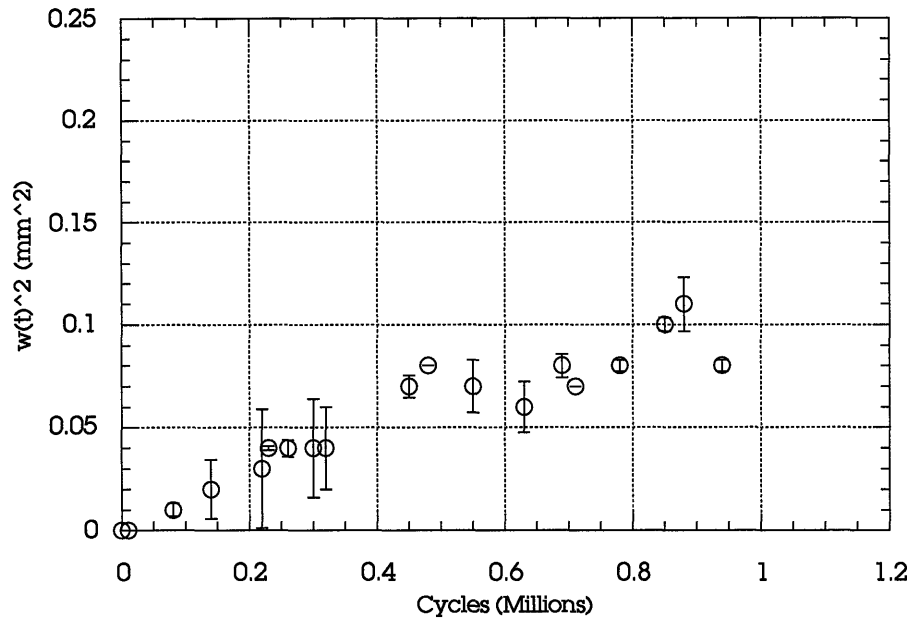


Figure 29: A plot of the seal wear squared showing the linear relationship between the wear that the seal experiences squared $[w(t)^2]$ and the number of cycles. The data shown are for the test with the CC#2 seal.

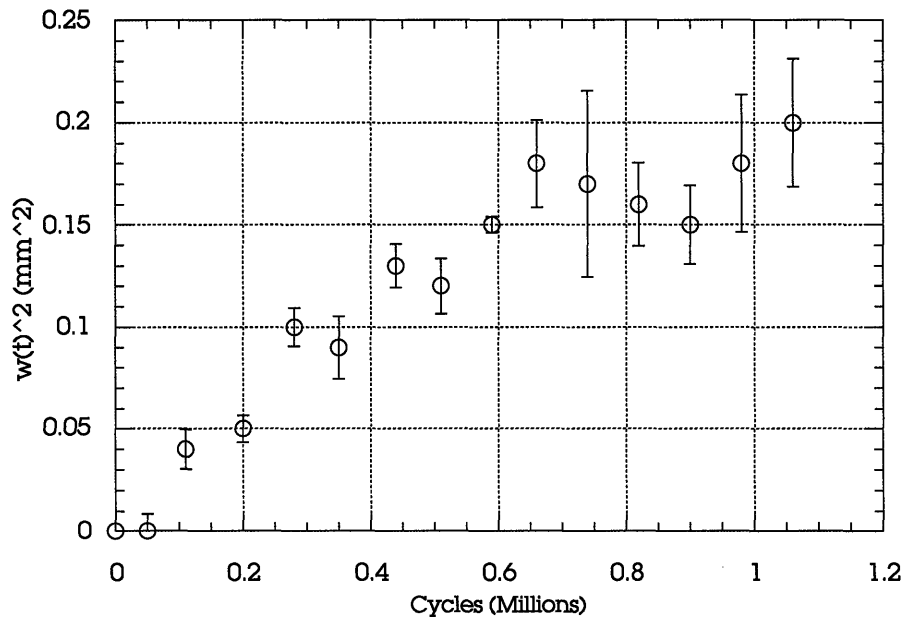


Figure 30: A plot of the seal wear squared showing the linear relationship between the wear that the seal experiences squared $[w(t)^2]$ and the number of cycles. The data shown are for the test with the CC#1 seal.

$$w(t) = h_o - h(t) \quad (7)$$

$$\frac{dw(t)}{dt} = -\frac{dh(t)}{dt} \quad (8)$$

The data suggest a relationship where:

$$\frac{dw(t)}{dt} \propto \frac{h_o}{d(t)} \quad (9)$$

with a solution of the form,

$$w(t) = \sqrt{k h_o} \sqrt{t} \quad (10)$$

where h_o is the initial seal thickness, and k is the seal wear rate with units of length per unit time. Since time in this document is measured in millions of cycles, k will have units of millimeters per million cycles.

For the two seals the slope of the line in Fig. 27 & 28 represents $k \cdot h_o$. For Fig. 27 (CC#2, $h_o = 1.55$ mm) $k = 0.07$ mm per million cycles, and for Fig. 28 (CC#1, $h_o = 1.58$ mm) $k = 0.13$ mm per million cycles.

5.3 Wear Mechanism

The inverse relation between wear and the size of the seal band is most likely coupled to the fact that the pressure between the seal lip and the bushing is also inversely related to the seal lip contact area. This is a strong indication that the wear is directly proportional to the contact pressure between the seal and the bushing.

Furthermore, as the seal wears it relieves some the strain that is taken up by the load ring. A change of 0.1 mm in the thickness of the seal lip corresponds to a 2% change in the strain on the load ring. However, since the stress/strain relationship of the loading ring is unknown, the corresponding change in pressure due to seal erosion cannot be quantified other than to say that it goes down. With the total wear of a seal over a million cycles being between 0.2 and 0.7 mm, this can correspond to a change in strain of between 4 and 14%.

Another thing that is apparent from looking at the plots is that mud or other foreign particles become trapped between the seal and the bushing (see section 3.1.) This is most easily seen in Fig. 30 at around 0.8 million cycles. For the period of time of between 0.7 and 0.9 million cycles the readings of

seal lip wear reverse direction and start climbing down. After 0.9 million cycles the wear continues its upward climb. Because it is assumed that the seal lip does not spontaneously regenerate, the likely explanation for the reading is that particles become trapped between the seal and the bushing.

As to the nature of the trapped particles, all that can be said now is that they are likely to be a combination of pieces of the seal and mud. The evidence for this is the presence of mud and seal fragments in the oil drained from the bushing assembly after the experiment. In order for mud particles to be present in the oil, they would've had to make their way across the seal.

5.4 Surface Analysis

Fig. 16 shows the top of one a seal tested for half a million cycles without mud. The picture shows a band about 1 mm in height running along the top of the seal lip where the seal came in contact with the bushing. The darkening is made visible by the permanent plastic deformation caused by the contact. Except for the band and two small ($\approx 1\text{mm}$) indentation marks, the seal is undamaged.

Fig. 17 & 18 are for another seal worn simultaneously with the one described above (half a million cycles without mud.) In addition to some blistering along the top, the top picture show the same 1 mm contact band visible in Fig. 16. The bottom picture shows a groove 0.02 mm in height and a smaller contact band (only .83 mm.) Despite the blisters and groove, the change in seal thickness is likely due mostly to creep.

Fig. 19 & 20 show a seal tested with mud for half a million cycles. The top and bottom of the seal have contact band of 1.4 mm. Both top and bottom show a similar pattern of erosions composed of grooves and blisters. The outermost part of the lip shows an uneven and grainy pattern of seal material. This pattern is most likely due to a temperature increase caused by the seal being rotated against the bushing without oil.

Fig. 21 & 22 show a seal tested for approximately one million cycles with mud. The seal band here has grown from 1 mm to 2.7 mm. The same grainy pattern present in the outer part of the previous seal re-appears here just larger. The smooth portion on the inside shows some streaks. The likely cause of the streaks is the trapping of particles as the seal face rubs against the bushing.

Fig 23 & 24 show a seal tested for one million cycles with mud. The seal band here is 2.9 mm.

<page 48>

6. Conclusions

6.1 Summary of Work

A version of the seal test unit (called a *mud box*) was modified with the objective of performing *in situ* measurements of the thickness of track seals. The modifications involved introducing a set of thin metal rods to contact the back of the seal and the seal contact surface through one of the ends of the apparatus. The rods relayed the position of the seal and its thickness as the experiment was run .

Of the four experiments performed, one was carried out without mud, and three were carried out with. The seals tested with mud showed a greater material erosion than the seal tested without. The seal tested without abrasives only suffered a permanent plastic deformation (attributable to the visco-elastic nature of the seal material) but no significant loss of thickness due to material erosion.

The data collected were matched to a model that predicts that the rate of seal erosion is directly proportional to the contact pressure between the seal and the bushing. The data also provide strong evidence that particles become trapped between the seal and the bushing.

6.2 Summary of Results

1. *Seal Plastic Deformation:* Seals tested without mud will undergo a permanent plastic deformation of between 0.07 to 0.11mm. For an average seal lip thickness of 1.55 mm, this corresponds to 6% of the seal lip thickness.

2. *Seal Erosion*: Seals tested with mud erode at a rate inversely proportional to the contact surface with the bushing. The experiments performed do not yet provide enough data to quantify precisely the wear rate, but two experiments yield wear formulas of the form:

$$w(t) = \sqrt{k h_0} \sqrt{t}$$

where h_0 is the initial seal thickness (typically on the order of 1.55 mm), k is between 0.7 and 0.13 mm per million cycles, and t is operating time in million of cycles.

6.3 Other Observations

1. *Placement of Probe*: The probe made up of a set of steel rods only measured the thickness of the seal at one point along its periphery (the so called *top*.) Adding more probes to the end cap is unlikely to result in more accurate information about the wear rate of the seal because for all experiments so far, the wear at the top of the seal was as large or larger than that experience by the rest of the lip.
2. *Length of Test*: Test were run for half a million and a million cycles (7 and 14 days respectively.) The information obtained in the first 0.6 million cycles is indicative of the wear rate for the seal (see Fig. 29 & 30.)

6.4 Directions for Future Work

Future work on this project centers around establishing a more complete list of the factors that contributes to seal effectiveness and expanding on the experimental work done to date.

In this work seal failure was specified as the point at which the seal thickness falls below a given value. In the field, oil leakage is used as criterion for seal failure. Future work will need to account for oil leakage as part of the definition of seal failure.

Experimentally, there are both short and long term plans. In the short term modifications and additions to the current setup as well as the use of a new test apparatus are planned. The existing setup will be changed so that the seal thickness can be monitored continuously and a transducer will be added to measure the water content of the soil mixture. Measures of water

content will be used to establish the role of mud composition (if any) on the wear of the seal.

In the new apparatus, a seal can be tested while pressed against a transparent window. In this manner the contact band as well as any particles that may become trapped can be observed.

In the long term, a study of the load characteristics of the seal lip, the stiffener ring, and the load ring are planned. Finite element analysis of these elements and their movements will provide a better estimate of contact pressure and shear forces between the seal lip and the bushing. These estimates should clarify the effect of contact pressure on seal wear and yield information regarding the forces experienced by the lip surface. Of particular interest, is the study of small variations in the seal geometry (e.g., the lip angle) and their effect on seal performance.